ResearchGate

See discussions, stats, and author profiles for this publication at: https://www.researchgate.net/publication/49786880

Pressure- and Heat-Induced Insertion of CO2 into an Auxetic Small-Pore Zeolite

ARTICLE *in* JOURNAL OF THE AMERICAN CHEMICAL SOCIETY · FEBRUARY 2011

Impact Factor: 12.11 · DOI: 10.1021/ja109765d · Source: PubMed

CITATIONS
25

READS
31

6 AUTHORS, INCLUDING:

Yongjae Lee
Yonsei University
170 PUBLICATIONS **2,473** CITATIONS
SEE PROFILE

Zhenxian Liu
Carnegie Institution for Science
178 PUBLICATIONS **2,103** CITATIONS
SEE PROFILE

Thomas Vogt
University of South Carolina
360 PUBLICATIONS **9,239** CITATIONS
SEE PROFILE

Available from: Thomas Vogt
Retrieved on: 01 February 2016

Pressure-Induced Argon Insertion into an Auxetic Small Pore Zeolite

Yongjae Lee,[†] Joseph A. Hriljac,[‡] and Thomas Vogt*[,§]

Department of Earth System Sciences, Yonsei University, Seoul 120-749, Korea, School of Chemistry, University of Birmingham, Birmingham, B15 2TT, U.K., and NanoCenter and Department of Chemistry and Biochemistry, University of South Carolina, 1212 Greene Street, Columbia, South Carolina 29208

Received: November 25, 2009; Revised Manuscript Received: January 23, 2010

We report that natrolite, $Na_{16}Al_{16}Si_{24}O_{48}\cdot 16H_2O$, a small pore auxetic zeolite can incorporate significant amounts of Argon under moderate pressure- and temperature conditions resulting in $Na_{16}Al_{16}Si_{24}O_{80}\cdot 16H_2O\cdot 6Ar$. This material has a ~6.5% larger unit cell than natrolite at ambient conditions and its structure is related to $Na_{16}Al_{16}Si_{24}O_{80}\cdot 24H_2O$, an intermediate superhydrated natrolite referred to as para-natrolite. Argon insertion under pressure into auxetic frameworks such as natrolites is an important and overlooked confinement mechanism with potential applications and implications.

Introduction

Aluminosilicate zeolites have framework structures based on connected AlO_4/SiO_4 tetrahedra with open channels and nanometer-size pores that contain charge-balancing cations (i.e., Ca^{2+}, Li^+, Na^+, K^+) and molecules or clusters of molecules such as water. Because of the reactant- and product selectivity during reactions taking place in their nanometer size cavities they have been labeled as "molecular sieves" and are recognized and being used as important industrial catalysts.[1,2] Furthermore, their cation and water exchange capabilities provide opportunities to tailor their physical and chemical properties and be useful in many applications such as radioactive and water waste management. Fascinating high pressure chemistry of microporous materials is currently being explored where both pressure-induced superhydration and pressure-induced amorphization[3,4] can occur depending upon the framework and conditions.

The structural response of zeolites to hydrostatic pressure was explored early on by Hazen,[5,6] who showed that the volume compressibility of zeolite Na-A (LTA), a material with nearly 50% of its unit cell volume empty depends on the pressure-transmitting medium used in a diamond anvil cell to ensure hydrostatic pressures. One explanation for this behavior was the pressure-induced insertions of molecular entities from the pressure-transmitting media. The first structural proof that pressure-induced hydration can lead to "superhydrated" zeolites was provided by Lee et al[7,8] using synchrotron powder diffraction to investigate small pore zeolite natrolite under pressure. These authors found that the ambient pressure phase $Na_{16}Al_{16}Si_{24}O_{48}\cdot 16H_2O$ can be superhydrated under pressure in the presence of water in the pressure-transmitting fluid. Water is selectively absorbed from the alcohol−water mixture and in the fully superhydrated state the material doubles its crystal water content to $Na_{16}Al_{16}Si_{24}O_{48}\cdot 32H_2O$. The crystallographic presence of excess water molecules and a description of the hydrogen-bonding network were later confirmed by high-pressure neutron powder diffraction.[9] The detailed structure of natrolite in a narrow pressure range between 1 and 1.5 GPa, which is related to a so-called Al,Si-ordered "paranatrolite" phase with an approximate formulas of $Na_{16}Al_{16}Si_{24}O_{48}\cdot 24\ H_2O$ and an ~7% larger unit cell volume compared to the ambient pressure phase and an ~4.5% larger one than the superhydrated phase after 1.5 GPa, is due to a framework distortion accommodating an intermediate with a less dense packing of the water molecules and is discussed in a more specialized paper (see Figure 2).[10] This paranatrolite phase $Na_{16}Al_{16}Si_{24}O_{48}\cdot 24H_2O$ then transforms into the superhydrated $Na_{16}Al_{16}Si_{24}O_{48}\cdot 32H_2O$ phase that has a smaller unit cell than the paranatrolite phase. The density of the superhydrated paranatrolite phase is lower than both $Na_{16}Al_{16}Si_{24}O_{48}\cdot 16H_2O$ and $Na_{16}Al_{16}Si_{24}O_4\cdot 32H_2O$ due to a 7-fold coordination of Na^+ cations and alternating two μ_2-water ligands bridging two Na^+ cations (see Figure 2 of this paper and Figure 3 of ref 9 for more details). In the fully superhydrated phase, only one μ_2-water bridge is present leading to a larger Na^+-Na^+ distance and a more compact structure with a smaller unit cell volume.

The atomistic mechanism of pressure-induced hydration (PIH) deduced from our crystallographic studies on natrolites reveals that under pressure the channels through which water can diffuse open up due to the antirotation of T_5O_{10} units composed of SiO_4 and AlO_4 or GaO_4 tetrahedra connected by oxygen "hinges" (Figure 1). Baur[11,12] categorized flexible frameworks as either "collapsible" or "noncollapsible" depending on whether the hinges corotate in the same (collapsible) or opposite (noncollapsible) directions. Such a "rotating squares"-mechanism[13] based on rigid tetrahedral units and "soft hinges" leading to a pore- and volume expansion and concomitant pressure-induced hydration (see Figure 1) has been independently discussed in the literature as one of the ways that auxetic behavior of materials manifests itself at the atomistic scale.[14] Auxetic materials are materials with negative Poisson's ratios that lead to a thinning of material when compressed or fattening when stretched in a perpendicular direction.[15,16] Recently Grima et al[17] showed experimentally that natrolite is indeed an auxetic zeolite with negative Poisson ratios. Thus our experimental observation of pressure-induced hydration can be rationalized by the "rotating-squares" mechanism as a consequence of the auxetic behavior of the natrolite framework.

The PIH water confinement mechanism might have significant geochemical implications as the example of the aluminosilicate laumonite shows. Laumonite's distribution is the Earth's crust

* To whom correspondence should be addressed.
[†] Yonsei University.
[‡] University of Birmingham.
[§] University of South Carolina.

10.1021/jp911231p © 2010 American Chemical Society
Published on Web 03/26/2010

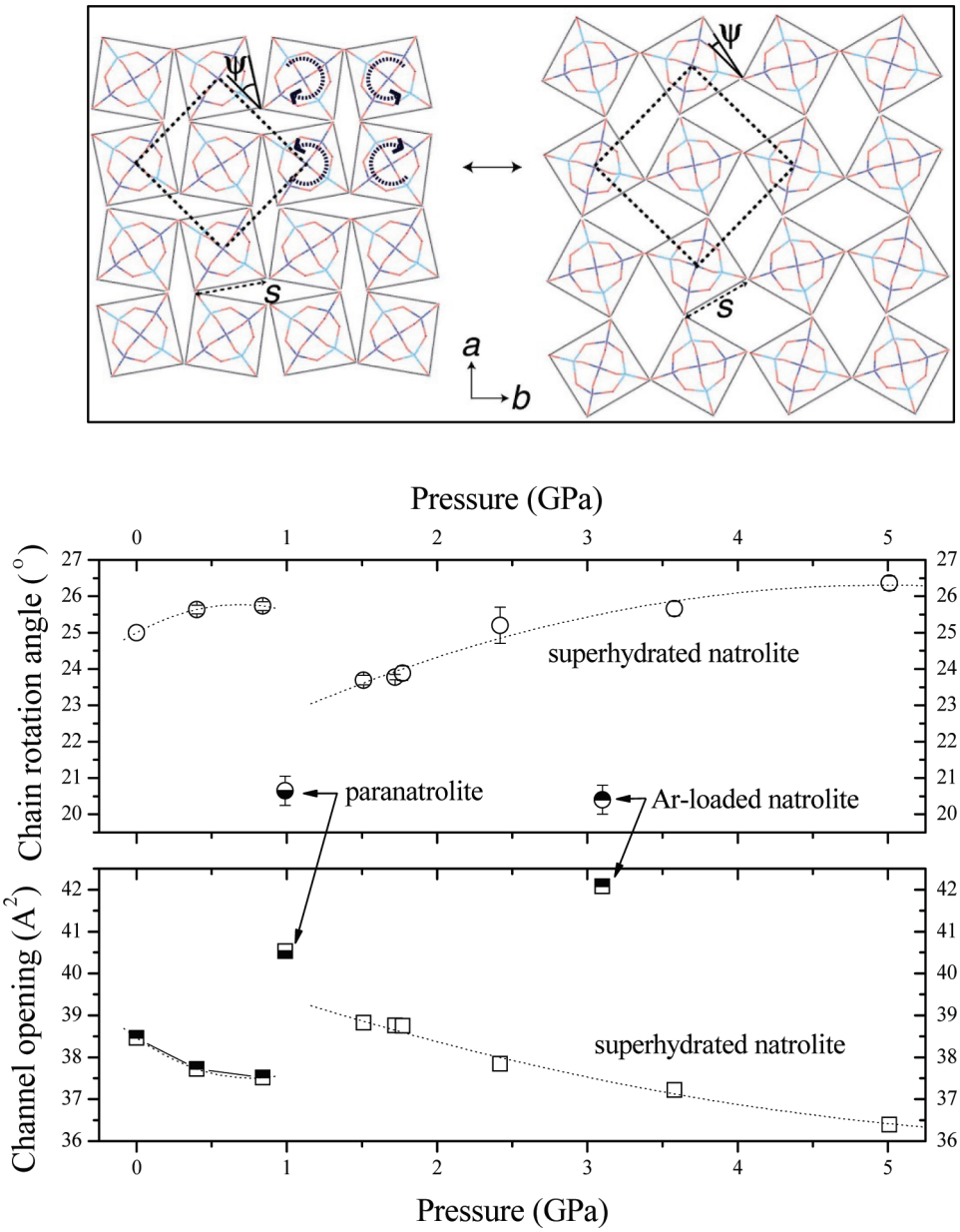

Figure 1. The variation of the chain rotation angles (Ψ) and channel openings (Å^2) under pressure in natrolite. Values for paranatrolite and Ar-loaded natrolite are shown in lower- and upper-half filled symbols, respectively. The top figure illustrates the concerted rotational behavior of the framework occurring in the plane perpendicular to the channel *c*-axis. Each square net represents dense T_5O_{10} unit, composed of Si (blue)-, and Al (cyan)-tetrahedra, connected by oxygen (red) hinges. The channel opening is defined by the chain rotation angle (Ψ) and the rigid T_5O_{10} unit edge length (*s*). Dotted lines show 2D unit cells and arrows indicate the cooperative chain rotation.

is often used as a thermobarometric indicator to infer conditions in fossil and active diagenetic and geothermal systems.[18] If formed in petroleum reservoirs it reduces porosity and permeability and thus diminishes production rates.[19] At humidities below 60% and room temperature, laumonite transforms to partially dehydrated laumonite, sometimes referred to as leonhardite.[20] At pressures of ∼2 kbar in the presence of water, a unit cell volume increase of ∼2.6% and a rehydration to a laumonite structure containing 18 water per formula unit occurs. Modeling of pressure-induced hydration in the aluminosilicate laumonite[21] $Ca_4Si_{16}Al_{18}O_{48}\cdot 18H_2O$ was followed by experimental work confirming PIH and a reversible disorder−order transition where at pressures above 4 GPa a 1 × 3 × 1 super structure is formed implicating an ordering of Ca cations and water. This super structure transforms back to the disordered parent structure after pressure release.[22] Neuhoff and Bird[23] had earlier proposed that the zeolite laumonite ($Ca_4Si_{16}Al_{18}O_{48}\cdot 18H_2O$) is actually superhydrated "leonhardite" ($Ca_4Si_{16}Al_{18}O_{48}\cdot 14H_2O$). We could experimentally confirm this hypothesis. This has important implications for rock permeability and petrology since calculations wrongly predict that assemblages containing superhydrated laumonite are stable at lower temperatures.

In the following, we report on a related phenomenon, the pressure-induced insertion of the noble gas argon into the framework structure of natrolite, an auxetic small pore zeolite. The noble gases He, Ar, Ne, Kr, and Xe are currently understood to originate from accreting planetessimals, which are the Earth's primordial building blocks. They are initially dissolved in silicate melts at high pressures in the Earth's mantle and ascend to the surface, where they are released into the atmosphere. Noble gases have a very stable electronic configuration and are therefore widely seen as nonreactive elements. However, the amount of Xe present in the atmospheres of the Earth and Mars is depleted by about a factor of 20 relative to the other noble

gases.[24] This is referred to as the "missing Xe problem" and one hypothesis suggests that Xe under certain conditions becomes soluble and/or forms compounds with minerals. It has been established that Xe can form water clathrates at ambient[25] and high-pressure conditions[26] and can be contained in the nanometer size pores of certain zeolites.[27] Work by Sanloup et al.[28] suggests the formation of Xe silicates at high pressures and temperatures based on laser-heated samples of Xe and β-cristobalite contained in diamond-anvil cells. In more recent work, evidence was put forward that Xe can be substituted into the silicon sites of the quartz structure.[29] The valence electrons of argon compared to the heavier noble gases are not screened very well by the core electrons and only one compound (HArF) has been experimentally established using low-temperature infrared spectroscopy.[30] Argon will not engage in any directional bonding interactions when absorbed into microporous materials but interact only via short-range van der Waals forces.

It has generally been postulated that noble gas atoms are dissolved into "holes" or interstitial sites of the three-dimensional network of silicate melts, thus relating the solubility to the presence of geometrically appropriate sites.[31−34] Experiments by Chamorro-Perez[35] probing the pressure-dependent solubility of Ar in SiO_2 melts revealed an increasing solubility up to pressures of about 5 GPa, corresponding to depths of less than 150 km in the Earth's mantle, followed by a reduced solubility above this pressure. The authors suggest that this behavior is due to changes in the structure of the SiO_2 melt near 5 GPa. While these results have been somewhat questioned by Schmidt et al[36] a threshold concentration of the solubility of both Ar and Xe in haplogranitic and tholeiitic melts has also been confirmed by these authors. Work again by Chamorro-Perez et al[37] found a similar behavior for the Ar solubility in olivine melts. A simple interpretation of this behavior based on "ionic porosity" assumes that available sites are never completely filled and the drop in Ar solubility is due to reduced access to "holes" by the densification of framework structures at higher pressures. We have expanded on our earlier work on pressure-induced hydration to search for evidence of pressure-induced insertion of argon into small pore zeolites and using in situ X-ray powder diffraction techniques under pressure have now characterized the reversible formation of a natrolite-containing significant amounts of Ar with the approximate general formulas $Na_{16}Al_{16}Si_{24}O_{80}\cdot 16H_2O\cdot 6Ar$. Our experimental studies and preliminary structural models will hopefully lead to more theoretical modeling and simulation of pressure-induced insertion of atomic and molecular species into structurally ordered as well as less ordered materials such as silicate melts.

Results and Discussion

Variable-pressure X-ray powder diffraction measurements were performed at beamline X7A of the National Synchrotron Light Source (NSLS) using a diamond-anvil cell (DAC). A powdered sample of the mineral natrolite (from Dutoitspan, South Africa, EPMA: $Na_{16}Al_{16}Si_{24}O_{80}\cdot 16H_2O$) was loaded into a 200 μm diameter sample chamber in a preindented stainless steel gasket, along with a few small ruby chips as a pressure gauge. The argon pressure medium was loaded into the sample chamber via the cryogenic method. The pressure the sample was exposed to was measured at room temperature by detecting the shift in the R1 emission line of the included ruby chips.[38] The cell was typically closed near 0.5 GPa and the pressure was then gradually raised in less than 0.5 GPa intervals. Diffraction data were collected at each measured pressure at room temperature with counting time of 3−5 h (3−35° in 2θ, λ = 0.6645(1) Å) using a horizontally focused (~200 μm) monochromatic X-ray provided by an asymmetrically cut bent Si (111) monochromator and a gas-proportional position-sensitive detector.[39] Near 3 GPa, a new phase with an expanded unit cell volume starts to form. The fact that we do not observe any structural changes below 3 GPa indicates that no significant water impurity detectable with diffraction techniques is present since this would lead to a the formation of para-natrolite $Na_{16}Al_{16}Si_{24}O_{48}\cdot 24H_2O$ and super hydrated phase $Na_{16}Al_{16}Si_{24}O_{48}\cdot 32H_2O$ as described above. Water is selectively absorbed from a 16:3:1 by volume mixture of methanol, ethanol, and water. We would expect water to also be selectively absorbed from an Ar−water mixture. During the initial pressure experiments, we observed a new phase near 3 GPa. However, a further increase of the pressure up to ~5 GPa does not lead to the complete transformation to a new phase. In a subsequent experiment, we therefore annealed the sample inside the pressure cell at ~3 GPa in an oven overnight at ~60 °C in an attempt to induce the complete transformation to the new high-pressure phase. In the presence of water, no thermal annealing was ever necessary to achieve superhydration. This new high-pressure phase with an expanded unit cell persisted up to ~5 GPa and does not exhibit any noticeable hysteresis upon pressure release. This is also in contrast to the superhydrated natrolite where, as indicated in Figure 3a, the paranatrolite phase can be stable at pressures near 0.5 GPa when releasing the pressure. The structural evolution of the natrolite-argon run was analyzed using Rietveld methods and the GSAS suite of programs.

The powder diffraction pattern measured at 3 GPa after cooling down the diamond anvil cell back to room temperature revealed a complete conversion of the original natrolite to the new phase which has a unit cell with an ~6.5% larger unit cell volume than the one of natrolite at ambient conditions. Intriguingly this unit cell volume is very close to the maximum expansion observed for water uptake under conditions suitable for pressure-induced hydration near 1 GPa where the so-called paranatrolite phase was found to have an ~7% larger unit cell than natrolite at ambient conditions.[10] Furthermore, the comparison of the channel opening and chain rotation angle at 1 and 3 GPa using alcohol−water and Ar as a pressure-transmitting medium, respectively, reveal very similar values (see Figure 1). The rotation angle Ψ of the fibrous chain, which is the mean of the angles between the sides of the quadrilateral around the T_5O_{10} tetrahedral building unit (T = Si, Al) projected on to the plane perpendicular to the channel,[40] also indicates the opening of the channel since the larger Ψ, the more elliptical the channel opening will be. Under PIH conditions the pressure range in which the ordered paranatrolite phase is stable is quite narrow and shows considerable hysteresis (se Figure 3a). Increasing the pressure leads to a superhydrated phase containing 32 water molecules per unit cell. Under pressurized Ar, the Rietveld refinement shows that approximately 6 Ar per formula unit are inserted into a site close to where excess water would be inserted in the case of PIH.

Other structural models locating Ar atoms in different sites or distributing them on different sites did either not improve the fit of the model to the experimental data or resulted in significantly worse fits. However, the error bar on the Ar site occupation is quite large due to the limited q-range of our data and the fact that we needed to introduce restraints when refining isotropic displacement parameters as indicated in Supporting Information, Table S1. Figure 2 reveals a comparison of the experimentally well-established superhydrated paranatrolite

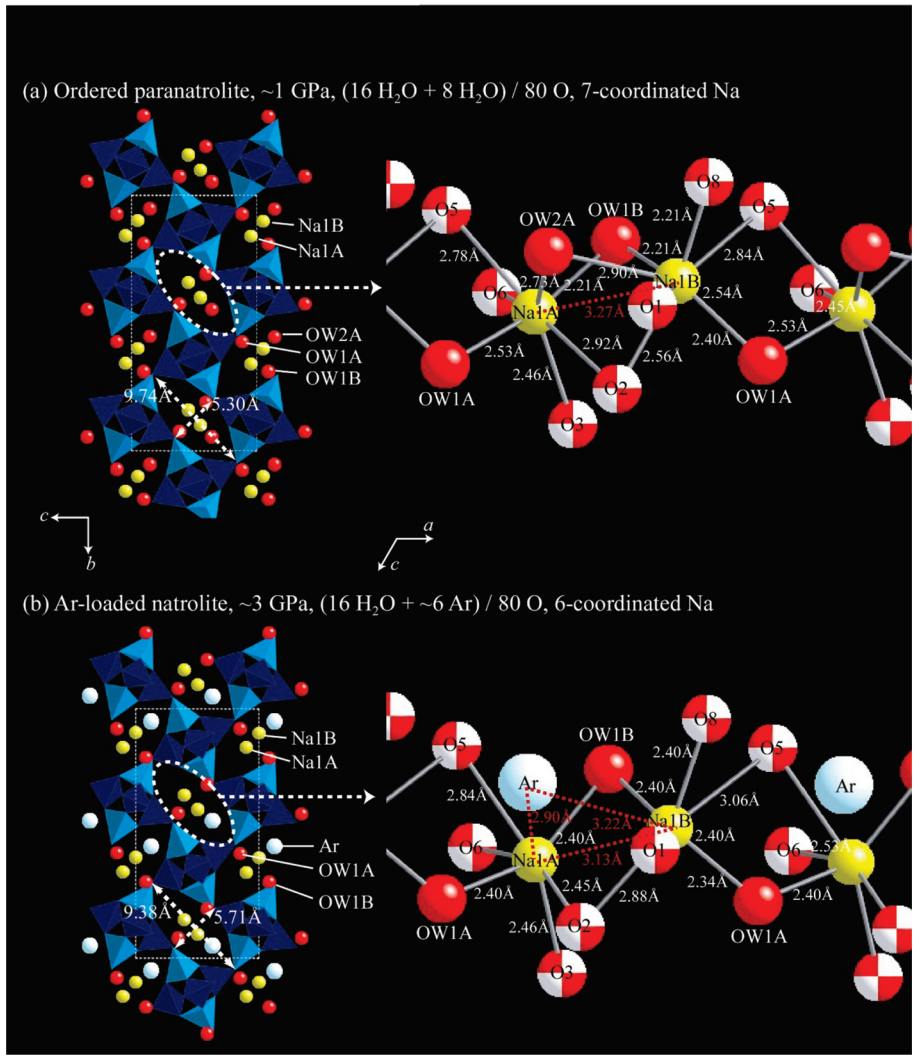

Figure 2. Pressure-induced insertion of (a) water at ~1 GPa and (b) argon at ~3 GPa into natrolite. Polyhedral representations are given parallel to the channel in the left, and expanded ball-and-stick models of the nonframework sodium cations and water/argon arrangements are shown perpendicular to the channel in the right. Data from Lee et al.[10] were used to represent the water-inserted structure. Tetrahedra are shown in two colors to illustrate the ordering of Al/Si over the framework tetrahedral sites. Yellow and white balls represent sodium and argon atoms, respectively, and oxygen atoms from water molecules and the framework are shown as red and red/white balls, respectively. The ellipticity of the channel opening is illustrated by the long and short framework oxygen distances across the channel. White dotted lines define the unit cells, and red dotted lines represent Na−Na and Na−Ar separation distances.

phases of $Na_{16}Al_{16}Si_{24}O_{80}\cdot 24H_2O$ and a highly constrained model for $Na_{16}Al_{16}Si_{24}O_{80}\cdot 16H_2O\cdot 6Ar$. The paranatrolite phases are structurally very similar. However, argon does not engage in any bonding interactions within the parantrolite structure and although short-range van der Waals interactions forces exist, it acts soley as a space-filling atom.

Further increase of the hydrostatic pressure in the presence of water leads to a complete hydration up to $32H_2O$ per formulas unit and a drop in the unit cell volume from 1.07 to 1.025 V_{Nat} with V_{nat} being the volume of the unit cell at ambient conditions. However, in the case of Ar insertion under pressures up to about 5 GPa we observe no discontinuity and no further insertion beyond the nominal composition of $Na_{16}Al_{16}Si_{24}O_{80}\cdot 16H_2O\cdot 6Ar$ (Figure 3). In the structure of the ordered paranatrolite phase $Na_{16}Al_{16}Si_{24}O_{80}\cdot 24H_2O$ formed by PIH, we have seven-coordinated Na^+ chains bridged by alternating distinct arrangements of two waters and one oxygen atom, and one water and one oxygen atom (see Figure 2). This leads to an overall shortening of the Na^+-Na^+ distances. Inserting additional water under pressure leads to the fully superhydrated phase containing 32 water where all Na^+ continue to be seven coordinated but now have the same arrangement of bridging ligands, one water and one oxygen, which results in a concomitant increase of the Na^+-Na^+ distance. The slightly larger Na^+-Ar distances (2.90(1) and 3.22(5) Å) compared to the Na^+-OH_2 ones with 2.73(5) Å and 2.90(5) Å result in almost the same chain rotation angle (Figure 1b) but a slightly higher unit cell volume. In the case of PIH, the transition to the fully superhydrated $Na_{16}Al_{16}Si_{24}O_{48}\cdot 32H_2O$ phase reduces the unit cell volume and increases the density. Structurally this denser structure is achieved by eliminating one of the μ_2-bridging water ligand between two Na+ cations while maintain the 7-fold Na^+. This leads to a larger Na^+-Na^+ distance due to the presence of now only one μ_2-bridging water ligand. At the same time, distances of the Na^+ to the inserted water are much shorter (2.53(5) Å) in the fully superhydrated $Na_{16}Al_{16}Si_{24}O_{48}\cdot 32H_2O$ than in the paranatrolite $Na_{16}Al_{16}Si_{24}O_{48}\cdot 24H_2O$ (2.73(1) Å and 2.90(5) Å), indicating a bonding interaction. Such a short Na^+-Ar distance is not possible. The intermediate paranatrolite structure is the only structural arrangement that can accommodate the larger Na^+-Ar distances required to host Ar within the pores of a natrolite-type structure.

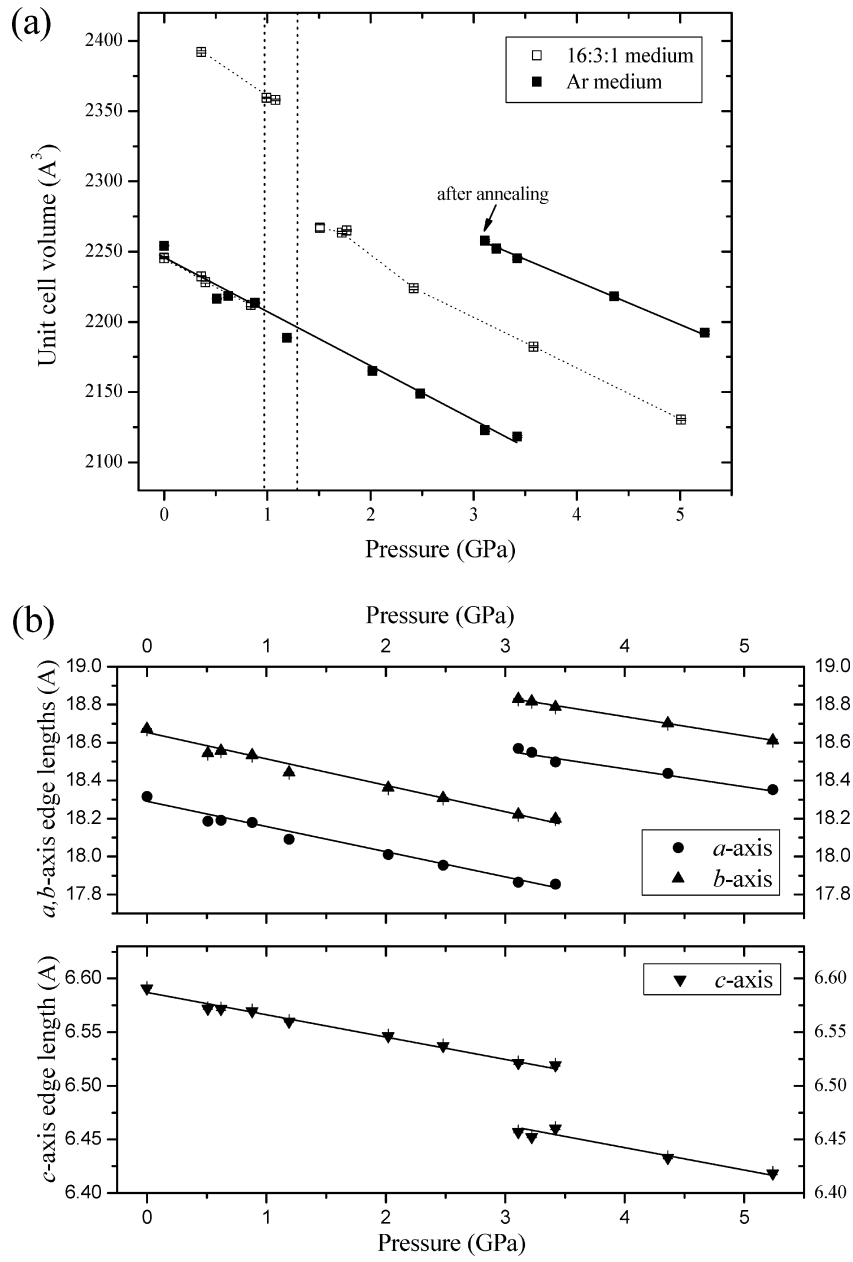

Figure 3. Pressure dependent changes of (a) the unit cell volume and (b) the unit cell edge lengths, normalized to the orthorhombic setting with 80 framework oxygen atoms, in natrolite ($Na_{16}Al_{16}Si_{24}O_{80}\cdot xH_2O$) under hydrostatic conditions mediated by argon pressure medium. Data from Lee et al.[8,10] were used to represent alcohol+water mixture run (open symbols) for comparison. The open symbols indicate that upon pressure-release there is a significant hysteresis and the paranatrolite phase containg water can be stable at pressures near 0.5 GPa.

In the structure of $Na_{16}Al_{16}Si_{24}O_{80}\cdot 16H_2O\cdot 6Ar$, the Na^+ remain 6-coordinated with the two distances between Ar and Na1A and Na1B being 2.90(1) and 3.22(5) Å, respectively. The sum of the ionic radii of 6-coordinated Na^+ (1.02 Å)[41] and the atomic radius of Ar (1.92 Å) indicates that the Na1−Ar distance we find is reasonable. In our model of the $Na_{16}Al_{16}Si_{24}O_{80}\cdot 16H_2O\cdot 6Ar$ phase the bond valence sums for both Na^+ cations are close to their nominal value. The Ar−O distances are all in the vicinity of 3.24 Å, which is a reasonable distance (1.92 +1.32 Å).

Conclusions

In this work, we have characterized a material, $Na_{16}Al_{16}Si_{24}O_{80}\cdot 16H_2O\cdot 6Ar$, which contains a significant amount of Ar inserted under moderate pressure and temperature in a structure that is related to an intermediate superhydrated structure. Unlike in the presence of water, further pressure-induced insertion of Ar in natrolite was not observed. During superhydration, the extra water is ultimately accommodated by a further structural rearrangement of the coordination sphere of the sodium atoms, and there is a substantial volume decrease due to the more efficient packing of the bonded water of the fully superhydrated phase. The argon atoms cannot form such a double-bridging arrangement and a more compact structure than the one related to the paranatrolite phase can therefore not be realized. The concerted behavior of the "antirotating squares" of T_5O_{12} units allowing this pressure-induced insertion due to its auxetic properties is similar to what has been observed in other important materials such as quartz and cristobalite.[42−45] Water and noble gas insertion under pressure into auxetic microporous materials is a novel and we believe an important confinement mechanism that might need to be taken into account

when modeling various geochemical and physical phenomena. Early modeling work by Grama[13] reveals that the "rotating-squares-model" allows for a good description of the auxetic behavior of natrolite and other members of the fibrous small-pore zeolites. However, in this and more recent work the modeling of auxetic behavior of natrolite $Na_{16}Al_{16}Si_{24}O_{48}\cdot 16H_2O$,[46] the transition to the para-natrolite phase $Na_{16}Al_{16}Si_{24}O_{48}\cdot 24H_2O$ and its subsequent transition to the fully superhydrated $Na_{16}Al_{16}Si_{24}O_{48}\cdot 32H_2O$ phase has never been investigated theoretically. The pressure-induced insertion of Ar to the paranatrolite phase $Na_{16}Al_{16}Si_{24}O_{48}\cdot 24H_2O\cdot 6H_2O$ could provide an opportunity to probe the first transition without having to take into account directional bonding interactions.

Pressure-induced insertions of molecules, ions and atoms have as outlined above implications for geochemical and physical modeling but could also have potential technological applications. Locating and containing both deuerated and tritiated water in aluminosilicates using PIH might be useful to manufacture targets for D-D and D-T laser-induced fusion. Incorporating under pressure radioactive and/or paramagnetic ions such as Gd^{3+} and Mn^{2+} in microporous materials which are subsequently trapped after pressure release might facilitate the oral use of these contrast agents for radiographic, CT and MRI-imaging in larger quantities and simultaneously reduce the health effects for patients since they can be excreted without being exchanging while in the body. Clearly finding systems where pressure-induced insertion takes place at lower pressures is the critical task for most envisioned applications. Modeling and understanding the relationship between auxetic behavior and pressure-induced insertion and trapping are vital to achieve this goal.

Acknowledgment. Y.L. and T.V. would like to acknowledge support from the Korean Science Foundation for a Global Research Laboratory on "Novel Nanotechnology using Pressure-Induced Auxetic Materials".

Supporting Information Available: Tables and figure. This material is available free of charge via the Internet at http://pubs.acs.org.

References and Notes

(1) Breck, D. W. *Zeolite Molecular Sieves: Structures, Chemistry and Use*; Krieger: Malabar, FL, 1984.
(2) Ming, D. W.; Allen, E. R.; Bish, D. L.; Ming, D. W. *Rev. Mineral. Geochem.* **2001**, *45*, 619.
(3) Greaves, G. N.; Meneau, F.; Kargl, F.; Ward, D.; Holliman, P.; Abergamo, F. *J. Phys.: Condens. Matter* **2007**, *19*, 415102.
(4) Chapman, K. W.; Halser, G. J.; Chupas, P. J. *J. Am. Chem. Soc.* **2009**, *131*, 17546–17547.
(5) Hazen, R. M. *Science* **1983**, 219.
(6) Hazen, R. M.; Finger, L. W. *J. Appl. Phys.* **1984**, *56*, 1838.
(7) Lee, Y.; Hriljac, J. A.; Vogt, T.; Parise, J. B.; Artioli, G. J. *J. Am. Chem. Soc.* **2001**, *123*, 12732.
(8) Lee, Y.; Hriljac, J. A.; Vogt, T.; Parise, J. B.; Artioli, G. J. *J. Am. Chem. Soc.* **2002**, *124*, 5466.
(9) Colligan, M.; Lee, Y.; Vogt, T.; Celestian, A. J.; Parise, J. B.; Marshall, W. G.; Hriljac, J. A. *J. Phys. Chem. B* **2005**, *109*, 18223.
(10) Lee, Y.; Hriljac, J. A.; Parise, J. B.; Vogt, T. *Am. Mineral.* **2005**, *90*, 252–257.
(11) Baur, W. H. *J. Solid State Chem.* **1992**, *97*, 243.
(12) Baur, W. H.; Joswig, W.; Muller, G. *J. Solid State Chem.* **1996**, *121*, 12.
(13) Grima, J. N.; Farrugia, P. S.; Caruana, C.; Gatt, R.; Attard, D. *J. Mater. Sci.* **2008**, *43*, 5962.
(14) Grima, J. N.; Jackson, R.; Alderson, A.; Evans, K. E. *Adv. Mater.* **2000**, *12*, 1912.
(15) Love, A. E. H. *A Treatise on the Mathematical Theory of Elsaticity*, 4th ed.; Dover: NY, 1944.
(16) Evans, K. E.; Nkansah, M. A.; Hutchinson, I. J.; Rogers, S. C. *Nature* **1991**, *353*, 124.
(17) Grima, J. N.; Gatt, R.; Zammit, V.; Williams, J. J.; Evans, K. E.; Alderson, A.; Walton, R. I. *J. Appl. Phys.* **2007**, *101*, 086102.
(18) Iijima, A. Development in Sedimentology. In *Diagenesis II*; Chilingarian, G. V., Ed.; Elsevier Science: Amsterdam, The Netherlands, 1988; Vol. 43, p 147.
(19) Crossey, L. J.; Frost, B. R.; Surdam, R. C. American Association of Petroleum Geologists Memoir. In *Clastic Diagenesis*; **1984**, Vol. 37, p 225.
(20) Artioli, G.; Smith, J. V.; Kvick, A. *Zeolites* **1989**, *9* (5), 377.
(21) White, C. L. I. M.; Lewis, D. W. *Angew. Chem., Int. Ed.* **2004**, *43*, 469–472.
(22) Lee, Y.; Hriljac, J. A.; Vogt, T. *Phys. Chem. Mineral.* **2004**, *31*, 421.
(23) Neuhoff, P. S.; Bird, D. K. *Mineral. Mag.* **2001**, *65*, 59.
(24) Anders, E.; Owens, T. *Science* **1977**, *198*, 453.
(25) Barrer, R. M.; Ruzicka, D. J. *Trans. Faraday Soc* **1962**, *58*, 2262.
(26) Dyadin, Y. A.; Larionov, E. G.; Mikina, T. V.; Starostina, L. J. *Mendelee Commun.* **1997**, *74*, 74.
(27) Heo, N. H.; Lim, W. T.; Kim, B. J.; Lee, S. Y.; Kim, M. C.; Seff, K. *J. Phys. Chem. B* **1999**, *103*, 1881.
(28) Sanloup, C.; Kemley, R. J.; Mao, H. *Geophys. Res. Lett.* **2002**, *29* (18), 30.
(29) Sanloup, C.; Schmidt, B. C.; Chamorro Perez, E. M.; Jambon, A.; Gregoryanz, E.; Mezouar, M. *Science* **2005**, *310*, 1174.
(30) Khriachtchev, L.; Pettersson, M.; Runeberg, N.; Lundell, J.; Räsänen, M. *Nature* **2000**, *406*, 875.
(31) Carroll, M. R.; Stolper, E. M. *Geochim. Cosmochim. Acta* **1991**, *55*, 211–225.
(32) Carroll, M. R.; Stolper, E. M. *Geochim. Cosmochim. Acta* **1993**, *57*, 5039–5051.
(33) Shibata, T.; Takahashi, E.; Matsuda, J.-I. *Geochim. Cosmochim. Acta* **1998**, *62*, 1241–1253.
(34) Shackelfor, J. F. *J. Non-Cryst. Solids* **1982**, *49*, 299–307.
(35) Chamorro-Perez, E.; Gillet, P.; Jambon, A. *Earth Planet. Sci. Lett.* **1996**, *145*, 97–107.
(36) Schmidt, B. C.; Keppler, H. *Earth Planet. Sci. Lett.* **2002**, *195*, 277–290.
(37) Chamorro-Perez, E.; Gillet, P.; Jambon, A.; Badro, J.; McMillan, P. *Nature* **1998**, *393*, 352–355.
(38) Bell, P. M.; Mao, H. K. *Carnegie Institute Washington Year Book*; Carnegie Institute: Washington, D.C., 1979; Vol. 78, p 665.
(39) Smith, G. C. *Synch. Rad. News* **1991**, *4*, 24.
(40) Baur, W. H.; Kassner, D.; Kim, C.-H.; Sieber, N. H. *Eur. J. Mineral.* **1990**, *2*, 761.
(41) Shannon, R. D.; Prewitt, C. T. *Acta Cryst. B* **1969**, 925.
(42) Yeganeh-haeri, A.; Weidner, D. J.; Parise, J. B. *Science* **1992**, *57*, 650.
(43) (a) Keskar, N. R.; Chelikowsky, J. R. *Nature.* **1992**, *358*, 222. (b) Keskar, N. R.; Chelikowsky, J. R. *Phys. Rev. B* **1993**, *48*, 16227.
(44) Smirnov, M. B.; Mirgorodsky, A. P. *Phy. Rev. Lett.* **1997**, *78*, 2413.
(45) Alderson, A.; Evans, E. K. *Phys. Rev. Lett.* **2002**, *89*, 225503.
(46) Gatt, R.; Zammit, V.; Caruana, C.; Grima, J. N. *Phys. Status Solidi* **2008**, *3*, 502–510.

JP911231P